3D Left Ventricular Modelling and Quantification from 2D Echocardiography Using Automated View Positioning

Vera H.J. van Hal[1], Debbie Zhao[1], Joshua R. Dillon[1], Gina Quill[1], Nicola C. Edwards[2,3], Robert N. Doughty[2,3], Alistair A. Young[1], and Martyn P. Nash[1,4]

[1] Auckland Bioengineering Institute, University of Auckland, New Zealand
[2] Green Lane Cardiovascular Service, Te Toka Tumai Auckland City Hospital, New Zealand
[3] Department of Medicine, University of Auckland, New Zealand
[4] Department of Engineering Science and Biomedical Engineering, University of Auckland, New Zealand
vera.van.hal@auckland.ac.nz

Abstract. 2D echocardiography (2DE) is the most widely used non-invasive cardiac imaging modality due to its availability and low cost. Using 2DE, cardiac function is assessed by combining information from different acquisition planes. However, these plane positions are unknown and therefore measurements of left ventricular (LV) mass, volumes, and ejection fraction rely on geometric assumptions. While cardiac magnetic resonance imaging (MRI) is the gold standard in assessing cardiac function, it is expensive and limited to major centres. To enable accurate LV assessment from 2DE, we trained a deep learning (DL) model to predict the position of 2DE views in 3D space and present a full pipeline for automated 3D LV modelling and quantification using registered 2DE acquisitions. Good view positioning of apical four-chamber and apical two-chamber views was obtained for 34 out of 38 subjects (89% feasibility). A comparison between LV volumes and masses derived from our model-based analysis of 2DE against gold standard MRI showed no significant differences in end-diastolic (ED) volume, end-systolic (ES) volume and ED mass, whereas significant underestimates of volumes and overestimates of masses were found using the guideline standard Simpson's Biplane Rule. Automated positioning of 2DE views in 3D space is feasible and important to overcome current geometrical assumptions in LV mass and volume estimation. This approach is readily available for clinical evaluation and applications involving cardiac digital twins.

Keywords: Echocardiography · Left Ventricular Quantification · Deep Learning · View Positioning · 3D Modelling

1 Introduction

Echocardiography (echo) remains the most widely used imaging modality to analyse cardiac function, due to its availability and low cost [9]. Using 2D

echo (2DE), cardiac function is assessed by combining information from multiple imaging planes. Simpson's Biplane Rule (SBR) is clinically recommended by international guidelines for estimation of volume, mass, and ejection fraction [9]. This method relies on blood-endocardial border delineations of two longitudinal acquisition planes; typically the apical four-chamber (A4C) and apical two-chamber (A2C) views [9]. However, SBR estimates of volume and mass rely on geometrical assumptions regarding the left ventricular (LV) orientation and cross-sectional shape, since plane positions are unknown [8]. While cardiac magnetic resonance imaging (MRI) is the gold standard for assessing cardiac function, it is comparatively expensive, only accessible in major centres, and limited by patient factors such as claustrophobia, heart rhythm and older metallic devices. In comparison to MRI, 2DE SBR is known to underestimate and overestimate LV volumes [2, 11] and masses [1]. There is a critical need to improve the accuracy of LV assessment from 2DE, as it plays a central role in clinical decision-making and longitudinal patient follow-up.

To overcome these limitations, previous research has focused on reconstructing the 3D LV shape from 2DE to enable both qualitative and quantitative assessment of heart structure and function [7, 10]. However, existing methods for 3D cardiac reconstruction using only 2D views are limited in accuracy [14]. Including view position information has been shown to improve the accuracy of 3D reconstruction to support clinical quantification and tasks, particularly for pathological cases [14]. Learning view positions from 2DE has shown to be feasible by simulating 2DE slices from 3D heart shape models [3] or by directly slicing 3DE images [5, 12, 15]. In Freitas et al. [3] and Iijima et al. [5], LV meshes were fitted to registered 2DE data, but none of these studies directly compared the 3D models and associated volume and mass estimates to those derived from gold standard MRI.

In this study, we aimed to perform accurate automated view positioning using standard A2C and A4C views. We train a deep learning (DL) model [15] for estimating 2DE view positions in 3D space by leveraging simulated 2DE views from slicing 3DE images and their associated ground truth view positions. Additionally, we combined the 2DE views with corresponding segmentations of the LV, which are obtained from registered LV meshes [17], to inform the DL model for optimal view alignment. The trained model is subsequently evaluated for the alignment of standard A2C and A4C views. It allows for the creation of LV shape models from registered and automatically segmented 2DE views. We leverage a dataset containing paired echo and cine MRI acquisitions from 190 volunteers. This gives the unique opportunity to compare LV shape models created from registered 2DE views to those created from gold standard MRI. We investigate the feasibility in creating these LV shape models from registered A4C and A2C views, evaluate the accuracy of volume and mass estimates in comparison to MRI, and compare performance to quantification using 2DE SBR.

2 Methods

We used the DL network PlaneInVol [15], which was initially developed for fetal brain ultrasound imaging, to predict the positions of 2DE views in 3D space. The method allows for an arbitrary number of input images and takes the relationship between them into account when predicting the location of each input image. We investigated the performance of this network for cardiac ultrasound imaging and present a full pipeline for automated 3D LV modelling using registered 2DE acquisitions. We use 3D LV modelling to calculate clinical indices, such as volumes and masses, and compare these values against clinical indices from MRI-derived LV models of the same subjects.

2.1 Multimodal image acquisition

The MITEA dataset [17], containing same-subject 3DE and cine MRI (<1h apart) from 152 participants (87 healthy subjects and 65 patients with a mix of cardiac diseases across varied demographics) was used for training and validation. The data was randomly divided into 122 participants for training (80%) and 30 participants for validation (20%). We prospectively acquired 2DE and MRI (<1h apart) from a further 38 subjects presenting for clinical MRI scans for testing, of which N=30 had confirmed cardiac pathology, and N=8 had no significant cardiac findings. Ethical approval was granted by the Health and Disability Ethics Committee of New Zealand (17/CEN/226), and written informed consent was obtained from each participant.

2.2 Training data generation

Slicing of the 3DE volumes was performed according to anatomical landmarks from the MRI-derived 3D LV models, which were registered to the 3DE image data according to the procedure described in Zhao et al. [17]. The long-axis of each LV model was extracted and used as a rotational axis along which simulated 2DE views were sampled. Random rotations were sampled on-the-fly, within a range between -40° and 160°. This includes the full 180° rotational degree-of-freedom (the opposite hemisphere was excluded because of rotational symmetry), and accounts for variability in expected rotational angles due to the heart's intrinsic shape. The A4C view is positioned at around 0°, and the A2C view is at around 60°. To account for these variations, a span of ± 40° around these expected positions was included, based on findings from the literature [12]. Moreover, in order to simulate apical foreshortening and small variations of tilting and translation of the ultrasound probe from the LV axis, additional augmentations were included: translations of ± 20 mm from the LV axis, in-plane tilts of ± 30° and out-of-plane tilts covering 70% of the LV radius to the epicardium. Within these constraints, 50 simulated 2DE slices were randomly sampled from each 3DE image at the ED and ES time points, resulting in a total of 12160 simulated 2DE slices together with their ground truth positions for each epoch (Fig. 1). Each plane position was parameterised by the centre

and two corner points of the extracted plane. The intersections of the registered LV model and the simulated 2DE slice planes were used to extract MRI-derived contours. The resulting binary segmentations of the lumen and myocardium were added to the channel dimensions for each image. The extracted 3DE coordinates were subtracted by the 3DE coordinates of the A4C view, to be able to define the plane position with respect to a reference view that was consistent between subjects. This allowed for the combination of images and coordinates from different subjects within one batch and improved generalisation of the DL network.

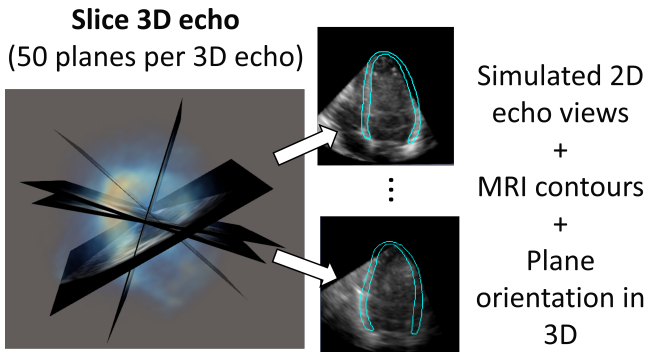

Fig. 1. 3DE sampling strategy for the creation of deep learning model training data. For each 3DE volume, 50 planes were randomly sampled (see text for constraints) according to anatomical landmarks. The simulated 2DE views, together with their image plane coordinates and corresponding MRI segmentations of the lumen and myocardium were used as input for the deep learning model.

The DL model was trained using a batch size of 250 and an initial learning rate of 10^{-4}, which was halved when the validation loss plateaued within 5 epochs. Contrast and brightness augmentations were applied with a probability of 30%. The validation loss represented the mean squared error between the predicted and ground truth centre and corner points of the plane. The model was trained for a maximum of 250 epochs and early stopping with a patience of 15 epochs. We used a single Tesla V100 PCIe GPU with a 32 GB RAM.

2.3 Automated 3D left ventricular modelling from 2D echo

The performance of the view positioning network was evaluated on 2DE images from 38 subjects. LV-focused A2C and A4C views at ED and ES were segmented using nnU-Net [4, 6] and used as input for the DL network. A bicubic Hermite and linear finite element model of the LV [16] was fitted to the resultant 2D segmentations in 3D space. Fig. 2 shows the automated LV modelling pipeline.

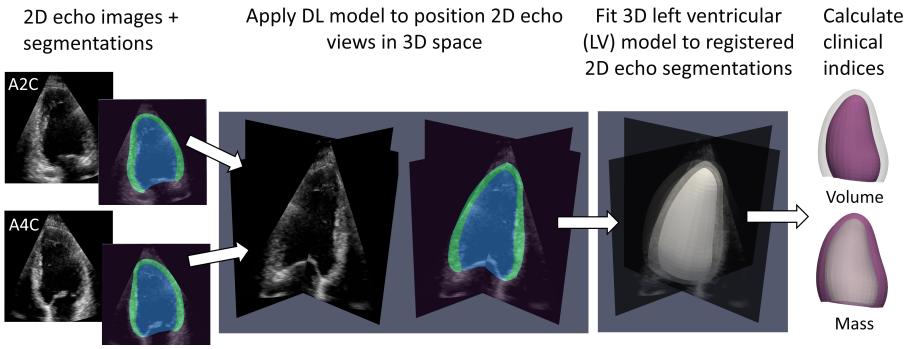

Fig. 2. Pipeline for automated 3D left ventricular modelling from 2DE images.

2.4 Evaluation metrics

The accuracy of the view positioning network was evaluated using the simulated 2DE views from 3DE images of the 30 subjects in the validation dataset. Only the 0° (A4C view) and 60° (A2C view) views were used as input, to mimic the limited availability of echo views in a clinical examination. Geometric accuracy is quantified using the Euclidean distance d_{3D} between the predicted (c_p) and ground truth (c_{GT}) centres of each slice, capturing translational errors. Rotational alignment is assessed using the geodesic distance θ_{3D} between the predicted (R_p) and ground-truth (R_{GT}) rotation matrices, providing a measure of angular misalignment in 3D space, described as:

$$\theta_{3D} = cos^{-1}\left(\frac{Tr(R_{GT} \cdot R_p^T) - 1}{2}\right) \tag{1}$$

Additionally, the Dice scores for the lumen and myocardium segmentations between the predicted slice locations and the ground truth slice locations were calculated.

For the evaluaton of 2DE alignment, no ground truth is available. However, the relative alignment of standard 2DE A2C and A4C views was evaluated by the Euclidean distance between the centres of the LV axes in the A2C and A4C views and the dot product of these LV axes. The LV axes were extracted from the nnU-Net segmentations of the A2C and A4C views, that were also used as input to the view positioning network. The base plane was defined as the border between the left atrium and LV segmentations. The apex was defined as the pixel in the LV segmentation that was the furthest away from the centre of the base plane. Consequently, the LV axis was defined as the line between these apex and basal points. The centre of the LV axis was defined as the mean of the apex and basal points. In this analysis, it is important to note that in a realistic scenario, perfect alignment of the LV axes between the A2C and A4C views is not expected, since small sonographer-dependent offsets in probe positioning can occur.

For each subject, the shape of the LV model fitted to the 2DE data was compared against the LV model fitted to the associated MRI. This was quantified by calculating the point-based error after rigid procrustes alignment of the 2D echo and MRI LV geometries. Finally, ED and ES volumes and mass were calculated using the LV models derived from the 2DE and MRI data to evaluate the performance of the automated view positioning pipeline on relevant clinical indices. The results from the LV modelling pipeline were also evaluated against volumes and masses from SBR using the 2DE nnU-Net segmentations.

3 Results

3.1 Performance on simulated 2D echo views from 3D echo

The performance on simulated 2DE views from 3DE was evaluated on the 0° (A4C) and 60° (A2C) views of the 30 subjects in the validation dataset. A mean centre distance error d_{3D} of 3.2 ± 1.8 mm and mean absolute rotation error θ_{3D} of 8.5° ± 4.4° were achieved. The mean Dice score between the extracted lumen and myocardium segmentations from the ground truth and predicted positions of the imaging planes were 0.88 ± 0.07 and 0.70 ± 0.15, respectively.

3.2 Performance on apical 2D echo views

Good 2DE view alignment results were obtained in 34 out of 38 subjects (89% feasibility). For the four cases with poor alignment, the predicted rotation an-

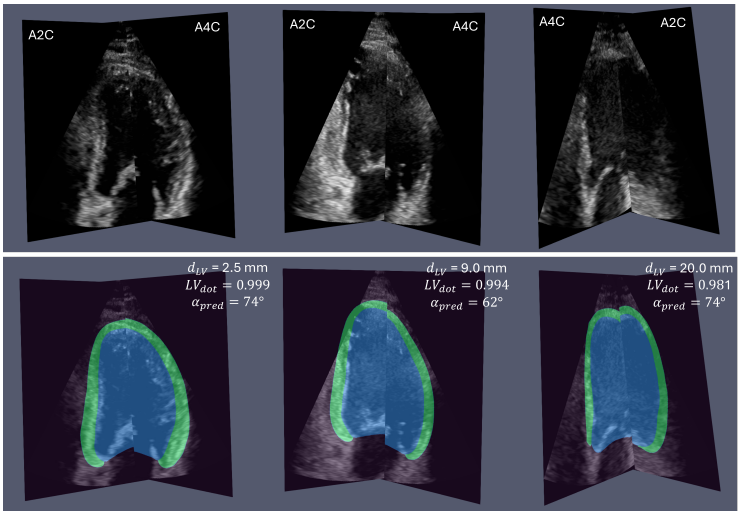

Fig. 3. Performance of the view positioning network on standard apical A2C and A4C views. Good (left), average (middle), and poor (right) image and segmentation alignment examples are shown together with corresponding LV centres distance (d_{LV}), dot products between LV axes (LV_{dot}) and predicted rotation angles between views (α_{pred}).

gles from A2C to A4C were still within anatomically plausible range, but the difference in LV axis location (measured by taking the average of the LV axis basal, centre and apex coordinates) was more than 2 cm between the two views, for either the ED or ES frame. The median and [IQR] rotation angles between the predicted A4C and A2C views for all 38 cases were 71° [58°, 77°] for the ED frames and 69° [60°, 76°] for the ES frames. The dot products between the LV axes from A2C and A4C were 0.981 ± 0.024 for the ED frames, and 0.991 ± 0.008 for the ES frames. The LV centre distances were 11.1 mm ± 5.4 mm and 8.0 mm ± 4.7 mm for the ED and ES frames, respectively. Fig. 3 illustrates examples of segmentation alignments for good, average, and poor cases among the 38 subjects.

3.3 Comparison against gold standard MRI and a clinical benchmark

Fig. 4 shows the average 2DE LV shape model from 38 subjects at ED and ES, overlayed with the average point-based distance between 2DE and MRI. It can be seen that the largest differences between the LV models fitted to 2DE and MRI can be found near the base. The mean ± SD Hausdorff distances were 14.3 mm ± 5.6 mm and 13.6 mm ± 3.2 mm at ED and ES, respectively. The mean ± SD point-based distances were 5.2 mm ± 1.7 mm at ED, and 5.1 mm ± 1.4 mm at ES.

Bland-Altman plots of the volumes and masses from LV models fitted to 2DE and MRI, as well as SBR versus MRI comparisons are shown in Fig. 5. The median values are also shown in Table 1. ED and ES volumes derived using conventional SBR analyses of 2DE were each significantly underestimated compared to gold standard MRI-derived values. Consequently, LV masses at ED and ES were significantly overestimated. In contrast, non-significant differences in ED and ES volumes and ED mass compared to MRI were found by fitting 3D LV models to the aligned 2DE images.

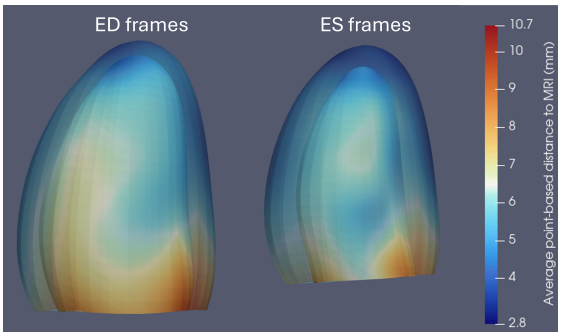

Fig. 4. Average point based alignment between LV models generated from 2DE and MRI (N=38). The side with the largest average point-based distances is shown.

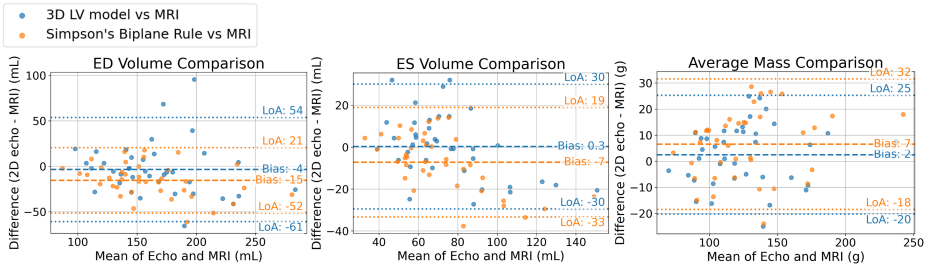

Fig. 5. Bland-Altman plots comparing volumes and masses between 2DE and MRI.

Table 1. Comparison of LV volumes and masses derived from 2DE using Simpson's Biplane Rule (SBR) and 3D LV modelling against gold standard measures from MRI. Median values and [IQR] are reported (N=38).

	SBR	**3D LV model**
ED LV volume difference (mL)	-16 [-27, -3]**	-6 [-24, 9]
ES LV volume difference (mL)	-6 [-15, 4]**	0 [-10, 11]
ED LV mass difference (g)	10 [-3, 21]*	2 [-9, 12]
ES LV mass difference (g)	2 [-2, 13]**	2 [-4, 11]*

** $p<0.001$, * $p<0.05$ (paired t-test vs MRI)

4 Discussion

We present a full pipeline for automated 3D LV modelling using standard apical 2DE views. We showed the feasibility of fitting 3D LV models to A4C and A2C views, which are routinely acquired in clinical practice. In doing so, the geometrical assumptions that are currently required for 2DE analysis are avoided, reducing the biases in volumes and masses compared to gold standard MRI.

The view positioning network achieved good 2DE alignment accuracy in 34 out of 38 subjects. The network was able to align the LV axes and myocardial structures between views and predicted rotation angles between A4C and A2C in accordance with existing literature [12]. In the other four subjects, the 2DE image quality was limited. In particular, for cases with shadowing artifacts around the apex in the A2C views or limited lateral wall contrast in both A4C and A2C views, the view positioning network was sometimes not able to align the A4C and A2C views correctly. Since our network was trained on simulated 2DE slices from 3DE, the network may have limited generalizability towards the artifacts and variability in image quality in routine 2DE acquisitions. Although we address this domain gap by adding binary segmentations of the lumen and myocardium in the image channel dimension, this could potentially be further improved by adding relevant ultrasound specific augmentations, such has hazing or shadowing artifacts, which have previously been shown to improve estimation of view position [12].

In the comparison between LV models fitted to 2DE and MRI data, the Bland-Altman plots show that, although the proposed method resulted in a substantially smaller bias, the limits of agreement (LoA) are in the same range or slightly larger compared to the use of SBR. However, the use of nnU-Net segmentations instead of manual contouring required by clinical 2DE analysis tools likely already reduces the bias and LoA in the calculation of volumes and masses using SBR. The large LoA for the ED frames were substantially reduced from [-61 mL, 54 mL] to [-54 mL, 30 mL] when excluding the four cases with poor view alignment from the comparison, indicating the large effect of these cases on the overall analysis. The alignment of the 2DE views was slightly better for the ES frames, possibly due to movement of the myocardium out-of-view during diastole, leading to less information in the ED frames compared to the ES frames. Fig. 4 shows that the largest differences in the LV models from 2DE and MRI can be found around the base. Although the point-based alignment shows average distances of around 5 mm, discrepancies in segmentation between 2DE and MRI at the base can lead to large differences in volumes and masses. In a previous comparison between 3DE and MRI, large mean regional surface distances were also found near the base, which can be explained by the reduced image resolution in these regions compared to the apex [18]. Moreover, inter-observer variability in CMR contouring is generally largest at the apex and the base [13]. Finally, there can be slight differences in timing between the ED and ES frames within the 2DE acquisitions compared to MRI, because of its limited temporal resolution. Hence, minor differences in shape can be expected at the base, because these regions deform the most during the cardiac cycle.

It may be possible to further improve the accuracy of the fitted LV models and subsequent clinical analysis by including more views, such as the apical three-chamber and parasternal short axis views. However, pairing of A4C and A2C already achieves high reconstruction precision for the LV at more than 95% in Wang et al. [14]. Future research could evaluate if downstream clinical indices further improve significantly when including more views.

The proposed view positioning network was evaluated using static ED and ES frames. This could be extended to include videos of the full cardiac cycle, since it can be expected that the temporal information provides added features that may help in the prediction of the echo view position in 3D space, particularly because structures can move in and out of view. At the same time, alignment of 2DE views over the full cardiac cycle is a challenging task, considering beat to beat variations and potential differences in relative view alignment during the cardiac cycle. The current study presents an important step towards the creation of dynamic 3D LV models, not only for clinical evaluation but also for applications involving cardiac digital twins.

5 Conclusion

Automatic positioning of 2DE views in 3D space is feasible, and 3D model-based interpretation can help to account for geometrical assumptions associated with

standard clinical methods for estimating LV mass and volumes. Future research will extend the current framework to span the full cardiac cycle.

Acknowledgments. This study was funded by the Health Research Council of New Zealand (Programme Grant 23/527). DZ is supported by a Pūtahi Manawa | Healthy Hearts for Aotearoa New Zealand Centre of Research Excellence Research Fellowship (Grant: FLW23-001). RD holds the New Zealand Heart Foundation Chair of Heart Health. AY is supported by the Engineering and Physical Sciences Research Council (Grant Number EP/Z533762/1).

Disclosure of Interests. The authors have no competing interests to declare that are relevant to the content of this article.

References

1. Chuang, M.L., Beaudin, R.A., Riley, M.F., Mooney, M.G., Manning, W.J., Douglas, P.S., Hibberd, M.G.: Three-dimensional echocardiographic measurement of left ventricular mass: comparison with magnetic resonance imaging and two-dimensional echocardiographic determinations in man. Int. J. Card. Imaging **16**(5), 347–357 (2000)
2. Cowie, B., Wright, L., Costello, B., Janssens, K., Howden, E., Flannery, D., Foulkes, S., Kluger, R., La Gerche, A.: Measurement of stroke volume with echocardiography compared to gold standard cardiac magnetic resonance imaging: an observational study. J. Cardiothorac. Vasc. Anesth. **37**(9), 1639–1645 (2023)
3. Freitas, J., Gomes-Fonseca, J., Tonelli, A.C., Correia-Pinto, J., Fonseca, J.C., Queirós, S.: Automatic multi-view pose estimation in focused cardiac ultrasound. Med. Image Anal. **94**, 103146 (2024)
4. Geven, B.W., Zhao, D., Creamer, S.A., Dillon, J.R., Quill, G.M., Edwards, N.C., Legget, M.E., Doughty, R.N., Young, A.A., Babarenda Gamage, T.P., et al.: Automated quality-controlled left heart segmentation from 2D echocardiography. Lect. Notes Comp. Sci. **14507**, 98–107 (2023)
5. Iijima, L., Luo, Y., Sesia, D., Kaura, A., Mayet, J., Yap, C.H.: Echopose: 6D pose estimation of sparse echocardiograms for left-ventricular 3D shape reconstruction. In: Proceedings IEEE CVPR. pp. 22753–22762 (2026)
6. Isensee, F., Jaeger, P.F., Kohl, S.A., Petersen, J., Maier-Hein, K.H.: nnu-net: a self-configuring method for deep learning-based biomedical image segmentation. Nature Methods **18**(2), 203–211 (2021)
7. Jansen, M.Z., Zhao, D., Ferdian, E., Creamer, S.A., Dillon, J.R., Verlyck, M.A., Quill, G.M., Edwards, N.C., Legget, M.E., Doughty, R.N., et al.: 3D left ventricular reconstruction from 2D echocardiograms for reliable volume estimation. Lect. Notes Comp. Sci. **15448**, 433–442 (2024)
8. Kim, W.J.C., Beqiri, A., Lewandowski, A.J., Puyol-Anton, E., Markham, D.C., King, A.P., Leeson, P., Lamata, P.: Beyond simpson's rule: accounting for orientation and ellipticity assumptions. Ultrasound Med. Biol. **48**(12), 2476–2485 (2022)
9. Lang, R.M., Badano, L.P., Mor-Avi, V., Afilalo, J., Armstrong, A., Ernande, L., Flachskampf, F.A., Foster, E., Goldstein, S.A., Kuznetsova, T., et al.: Recommendations for cardiac chamber quantification by echocardiography in adults: an update from the american society of echocardiography and the european association of cardiovascular imaging. Eur. Heart J. Cardiovasc. Imaging **16**(3), 233–271 (2015)

10. Laumer, F., Rubi, L., Matter, M.A., Buoso, S., Fringeli, G., Mach, F., Ruschitzka, F., Buhmann, J.M., Matter, C.M.: 2D echocardiography video to 3D heart shape reconstruction for clinical application. Med. Image Anal. **101**, 103434 (2025)
11. Lee, S., Chin, S.E., Nielsen, J.C., Roytman, Z., Ko, H.H., Lytrivi, I.D., Srivastava, S.: Comparison of two-dimensional echocardiography methods of ventricular volume quantification to cardiovascular magnetic resonance in left ventricular volume overload. Prog. Pediatr. Cardiol. **46**, 57–64 (2017)
12. Pasdeloup, D., Olaisen, S.H., Østvik, A., Sabo, S., Pettersen, H.N., Holte, E., Grenne, B., Stølen, S.B., Smistad, E., Aase, S.A., et al.: Real-time echocardiography guidance for optimized apical standard views. Ultrasound Med. Biol. **49**(1), 333–346 (2023)
13. Suinesiaputra, A., Cowan, B.R., Al-Agamy, A.O., Elattar, M.A., Ayache, N., Fahmy, A.S., Khalifa, A.M., Medrano-Gracia, P., Jolly, M.P., Kadish, A.H., et al.: A collaborative resource to build consensus for automated left ventricular segmentation of cardiac mr images. Med. Image Anal. **18**(1), 50–62 (2014)
14. Wang, Y., Xu, H., Lu, W.: Feasibility of whole heart 3D shape reconstruction from sparse echocardiographic views using ct-derived simulations. Sci. Rep. (2026)
15. Yeung, P.H., Aliasi, M., Papageorghiou, A.T., Haak, M., Xie, W., Namburete, A.I.: Learning to map 2D ultrasound images into 3D space with minimal human annotation. Med. Image Anal. **70**, 101998 (2021)
16. Young, A.A., Cowan, B.R., Thrupp, S.F., Hedley, W.J., Dell'Italia, L.J.: Left ventricular mass and volume: fast calculation with guide-point modeling on mr images. Radiology **216**(2), 597–602 (2000)
17. Zhao, D., Ferdian, E., Maso Talou, G.D., Quill, G.M., Gilbert, K., Wang, V.Y., Babarenda Gamage, T.P., Pedrosa, J., D'hooge, J., Sutton, T.M., et al.: Mitea: A dataset for machine learning segmentation of the left ventricle in 3D echocardiography using subject-specific labels from cardiac magnetic resonance imaging. Front. Cardiovasc. Med. **9**, 1016703 (2023)
18. Zhao, D., Quill, G.M., Gilbert, K., Wang, V.Y., Houle, H.C., Legget, M.E., Ruygrok, P.N., Doughty, R.N., Pedrosa, J., D'hooge, J., et al.: Systematic comparison of left ventricular geometry between 3D-echocardiography and cardiac magnetic resonance imaging. Front. Cardiovasc. Med. **8**, 728205 (2021)